AIAA

CELEBRATING THE EVOLUTION OF FLIGHT
1903 TO 2003 ... AND BEYOND

AIAA 2003-4190

Experimental Investigation of Supercritical Startup of a Nitrogen/Stainless Steel Cryogenic Heat Pipe

Paulo Couto
Federal University of Santa Catarina
Florianopolis,SC Brazil

Marcia B. H. Mantelli
Federal University of Santa Catarina
Florianopolis, SC, Brazil

Jay M. Ochterbeck
Clemson University
Clemson, SC, USA

36th AIAA Thermophysics Conference
23 - 26 June 2003
Orlando, Florida

AIAA 2003-4190

EXPERIMENTAL INVESTIGATION OF SUPERCRITICAL STARTUP OF A NITROGEN/STAINLESS STEEL CRYOGENIC HEAT PIPE

Paulo Couto*
Federal University of Rio de Janeiro – UFRJ (change to UFSC as work was done there)
Department of Mechanical Engineering - EE/COPPE, P.O. Box 68503
Rio de Janeiro, RJ, 21945-970, Brazil

Marcia B. H. Mantelli†
Federal University of Santa Catarina - UFSC
Department of Mechanical Engineering - EMC, P.O. Box 476
Florianopolis, SC, 88040-900, Brazil

Jay M. Ochterbeck‡
Clemson University
Department of Mechanical Engineering,.
Clemson, SC, 29634-0921, USA

Abstract

An experimental investigation of the supercritical startup of a nitrogen/stainless steel cryogenic heat pipe is presented. The experiments were conducted at the Satellite Thermal Control Laboratory of the Federal University of Santa Catarina – Brazil, during the year of 2002, as part of a program funded by the Brazilian Space Agency and the Brazilian Council for Research and Development. A detailed description of the experimental setup used is presented, and several data sets for the transient axial temperature distribution of the heat pipe are shown. A previously developed transient, one-dimensional model developed for microgravity is used to predict theoretically the internal vapor pressure and the working fluid mass distribution. The results showed that cryogenic heat pipes are very sensitive to external heat convection, even at rarefied external atmospheres, and the parasitic heat loads can change significantly the operational temperature of the cryogenic heat pipe. The effects of parasitic heat loads must be accurately considered during the design stages of this device. Also, the fluid charge plays an important role in the determination of the initial thermodynamic state of the cryogenic heat pipe.

Introduction

Heat pipes are highly reliable and efficient heat transfer devices employed in many terrestrial and space applications[1]. This device uses the latent heat of vaporization (condensation and evaporation) of a working fluid to transfer relatively large amounts of energy over a long distance with a small temperature drop. During normal operation, the working fluid remains in a saturation condition, with liquid contained in a wick structure and vapor in the core section. The saturated liquid evaporates in the evaporator section due to a heat input, and vapor flows towards the condenser section where it condenses. The difference in capillary pressure developed between the evaporator and condenser in the wick structure pumps the working fluid back to the evaporator section.

Cryogenic heat pipes are one of the many different existing types of heat pipes. Usually they operate at temperatures below 200 K and their operational temperature range from the triple point temperature to the critical temperature, which is relatively narrow for cryogenic fluids[2]. Different from low and medium temperature heat pipes, cryogenic heat pipes must start from a supercritical condition. The entire heat pipe must be cooled below the critical temperature of the working fluid for the proper operation. A liquid column develops in the wick structure due to the condensation process. As the temperature of the condenser decreases, the liquid column advances towards the evaporator end. The cooling effect of the liquid vaporization at the liquid column leading edge cools the dry length of the heat pipe, priming the wick structure until steady state operation is achieved[3].

Cryogenic working fluids usually exhibits very low values of surface tension and latent heat of vaporization, resulting in heat pipes with low heat transport capacity, which are very sensitive to parasitic heat loads[4], fluid charge[5] and acceleration fields.[6-8] The parasitic heat loads can change significantly the operational temperature of the cryogenic heat pipe, and may add loads to the heat pipe on the order of the maximum transport capability. In addition to imposing additional heat load, the parasitic heat leaks can adversely affect the transient start-up behavior for the system. The objective of the present paper is to investigate experimentally the startup process of a cryogenic heat pipe accounting for the effects of parasitic heat loads and fluid charge. To achieve the objective of this work an experimental setup was built at the Satellite Thermal Control Laboratory (NCTS) of the Federal University of Santa Catarina (UFSC), Brazil,

* Currently visitor professor at Federal University of Rio de Janeiro, Brazil. pcouto@ltte.coppe.ufrj.br, Member AIAA.
† Professor, marcia@emc.ufsc.br, Member AIAA.
‡ Associate Professor, jochter@ces.clemson.edu, Associate Fellow AIAA.

Conclusions

The experimental and theoretical data provided a good insight of the supercritical startup of cryogenic heat pipes and some conclusions are listed below:

1. Cryogenic heat pipes are very sensitive to parasitic heat loads. The rewetting process is controlled by the conducted heat flux from the dry region of the heat pipe. The parasitic heat loads increase the temperature gradient in the dry region, increasing the heat conduction to the liquid column. Also, parasitic heat loads vaporize the fluid along the liquid column edge, decreasing the average liquid velocity. These two effects combined decrease the liquid column momentum, and the rewetting process may stagnate before the heat pipe is fully primed for relatively small parasitic heat loads. Additionally, parasitic heat loads may add loads to the heat pipe on the order of the maximum heat transport capability.
2. An excess of fluid charge will cause an increase of the vapor pressure of the heat pipe. Depending on the combination of parasitic heat loads and excess of fluid charge, the vapor pressure may never decrease below the critical pressure of the working fluid, even if the condenser is at a temperature below the critical point. A deficiency of working fluid will decrease the vapor pressure during startup, but total amount of working fluid may not be enough to prime completely the heat pipe.
3. A fast cooling rate of the condenser will cause a large temperature gradient on the dry region of the heat pipe. As the heat pipe continues to cool down, the subcooled liquid will turn into saturated fluid at a temperature far below the critical point, which will produce a liquid column with a considerably large momentum, facilitating the priming of the heat pipe. A fast cooling rate may be considered for ground tests when a successful startup is required for heat transport tests of cryogenic heat pipes.

Acknowledgements

The authors would like to acknowledge the Brazilian Space Agency – AEB, CAPES Foundation, Brazilian Council of Research and Development – CNPq, Clemson University and the Federal University of Santa Catarina for supporting this project. The authors also would like to acknowledge the help of Flávio Reis, Guilherme Kratka and Fabricio Azevedo during the development of this work.

References

[1] Peterson, G. P., *An Introduction to Heat Pipes – Modeling, Testing and Applications*, John Wiley and Sons, Inc., New York, NY, 1991.

[2] Faghri, A., *Heat Pipe Science and Technology*, Taylor and Francis, Washington DC, 1995.

[3] Yan, Y. H. And Ochterbeck, J. M., "Analysis of Supercritical Start-Up Behavior for Cryogenic Heat Pipes", AIAA Journal of Thermophysics and Heat Transfer, Vol. 13, No. 1, pp. 140 – 145, Jan./Mar. 1999.

[4] Couto, P., Ochterbeck, J. M., Mantelli, M. B. H., "Analysis of Supercritical Start-up Limitations for Cryogenic Heat Pipes with Parasitic Heat Loads", AIAA Paper No. 2002-3095, June, 2002.

[5] Röster, S., Groll, M., Supper, W., and Konev, S., "Analysis and Experimental Investigation of a Cryogenic Methane Heat Pipe", Proc. of the 16th Intersociety Conference on Environmental Systems, pp. 352 – 355, San Diego, CA, July, 1986.

[6] Ochterbeck, J. M., Peterson, G. P., and Ungar, E. K., "Depriming/Rewetting of Arterial Heat Pipes: Comparison with Share-II Flight Experiment", AIAA Journal of Thermophysics and Heat Transfer, Vol. 9, pp. 101 – 108, No. 1, Jan./Mar., 1995.

[7] Joy, P., "Optimum Cryogenic Heat Pipe Design", ASME PAPER 70-HT/SpT-7, June, 1970.

[8] Peng, X., F., and Peterson, G. P., "Acceleration Induced Depriming of External Artery Heat Pipes", AIAA Journal of Thermophysics and Heat Transfer, Vol. 6, No. 3, pp. 546 – 548, 1992.

[9] Couto, P., and Mantelli, M. B. H., "Cryogenic Heat Pipe – A Review of the State-of-the-Art", Proc. of the Brazilian Congress of Thermal Engineering and Sciences, Vol. CD-ROM, Porto Alegre, RS, Brazil, Oct., 2000.

[10] Brazilian Space Agency, *PNAE – Brazilian Policy for Space Activities* (original in Portuguese), Published by AEB, Brasilia DF, Brazil, 1996.

[11] Colwell, G. T., "Prediction of Cryogenic Heat Pipe Performance", NASA Final Report NSG-2054, Mar. 1977.

[12] Brennan, P. J., Thienen, L., Swanson, T., and Morgan, M., "Flight Data for the Cryogenic Heat Pipes (CRYOHP) Experiment", AIAA Paper No. 93-2735, Jul. 1993.

[13] Rosenfeld, J. H., Buchko, M. T., and Brennan, P. J., "A Supercritical Start-Up Limit to Cryogenic Heat Pipes in Microgravity", Proc. of the 9th International Heat Pipe Conference, Vol. 2, pp. 742 – 753, Albuquerque, 1995.

[14] Couto, P., *Theoretical and Experimental Analysis of Supercritical Startup of Cryogenic Heat Pipes*, Ph.D. Thesis, Mechanical Engineering Dept., Federal University of Santa Catarina, Florianópolis, Brazil, Mar. 2003.

[15] Jacobsen, R. T., Penoncello, S. G. and Lemmon, E., "Thermodynamic Properties of Cryogenic Fluids", 1st Edition, New York, NY: Plenum Press, 1997.

saturation level provides a saturated liquid with a small latent heat and very low surface tension, which makes it very sensitive to parasitic heat loads;

With increased vacuum level, contact resistance effects between the brass sleeves and the calorimeter provided less cooling capacity of the experimental apparatus. This can be verified as follows: the pressure inside the vacuum chamber during this supercritical startup experiment was 2×10^{-2} mbar, or 100 times lower than the pressure of the first experiments. In this rarefied atmosphere any effect of convection over the heat pipe startup can be neglected. With low vacuum level on the first tests, the atmosphere inside the vacuum chamber was cooled by the calorimeter, which has a large thermal mass, improving the heat transfer from the calorimeter to the sleeve, and to the heat pipe condenser.

To check this explanation, the rotary pump of the vacuum chamber was turned off after the non-operational condition was achieved. The pressure in the vacuum chamber increased quickly to 6×10^{-2} mbar in less than one minute, to 2×10^{-1} mbar in five minutes, and to 1 mbar after 15 minutes remaining stable around this value for one hour. The temperature profiles of the heat pipe for this test are shown in Fig. 14. It can be observed that the local temperatures of the heat pipe decreased after the shut down of the rotary pump due to improved convection inside the vacuum chamber. At cryogenic levels of temperature, the heat pipe is very sensitive to small heat loads, even those provided by a rarefied atmosphere.

A 5th test (test V) followed test IV, on the October 4th 2002, with the same setup. The same startup failure was observed showing that the calorimeter was not able to provide enough cooling to the condenser regions of the heat pipe. The experiment presented good repeatability. After test V, the experimental setup was disassembled. The heat pipe was vented and a new calorimeter was designed. The new calorimeter allowed the liquid nitrogen to be in direct contact with the condenser wall of the cryogenic heat pipe, thus providing a larger cooling capacity.

A last experiment (test VI) was performed using a new calorimeter. The new calorimeter provided enough cooling to the heat pipe and an "almost" successful startup was obtained, with 97% of the total length primed by the liquid column. The heat pipe did not prime completely because there was still a parasitic heat load incoming from the filling valve. However, the calorimeter imposed an abrupt cooling of the condenser, producing a fast transient: according to the experiment the heat pipe was primed in less than 15 minutes (it means a variation of 14 K per second in the condenser section, and a 0.2 K per second in the evaporator end). The numerical solution of the model was not able to reproduce the fast transient due to the large temperature gradient at the leading edge of the liquid column caused by the abrupt cooling of the condenser region. As the temperature of the condenser decreased quickly, the theoretical average liquid column velocity increased quickly, which in turn, provided a long liquid column length. The long length obtained produced a large temperature gradient at the liquid column interface, which pushed back the liquid column, causing the iterative process to diverge. Several time steps as small as 0.1 sec. were tried, but the model took almost 1 minute to solve this small time step before the divergence to occur. Therefore, no comparison between theoretical and experimental data was possible for this experiment. Figure 15 shows the transient cool-down experimental data. The condenser region was cooled to the critical temperature of the nitrogen in less than 3 minutes, and the cooling effect spread over the heat pipe in less than 15 minutes. The heat pipe reached a steady state after 45 minutes of testing, with the condenser region at a temperature around 80 K, and the remaining length at 108 K. The fill valve was at 125 K.

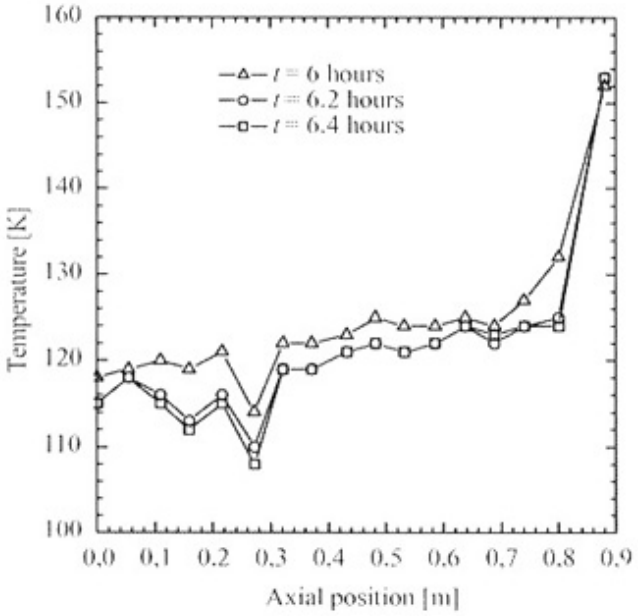

Figure 14. Temperature profiles after rotary pump shut down (test IV).

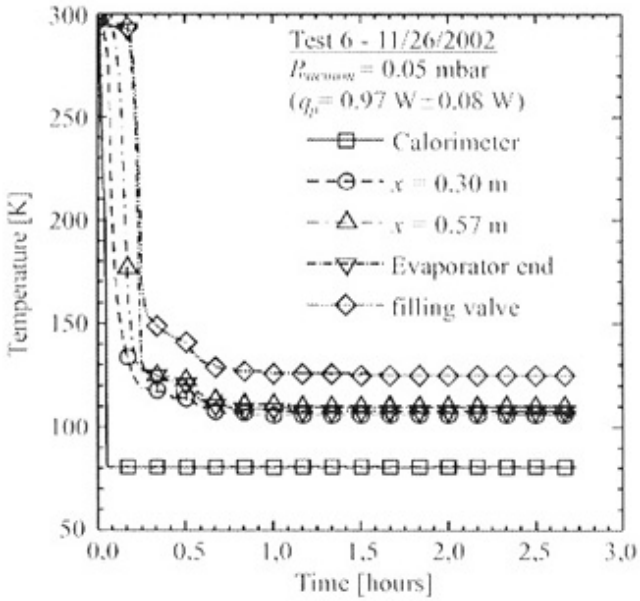

Figure 15. Transient cool-down (test VI).

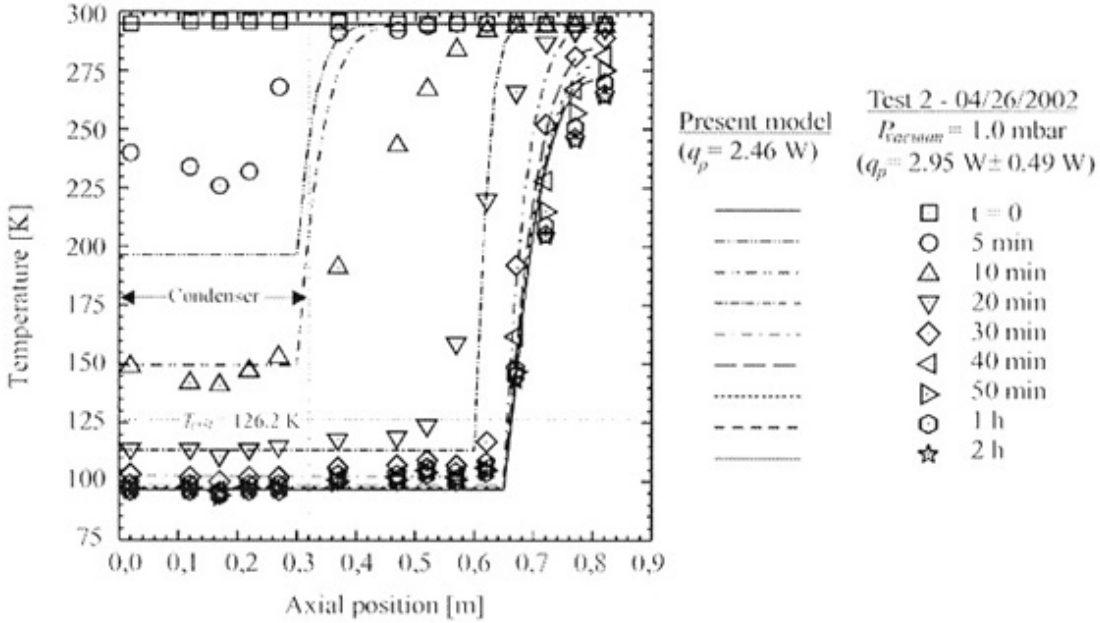

Figure 11. Temperature profiles (test II).

test. As the filling valve was not covered with MLI, there was a "leak" of parasitic heat load from the valve to the experiment. To account for this parasitic heat load, experimental data of the temperature of the filling valve and of the evaporator end were used to estimate the conductive heat load coming from the valve. This conductive parasitic heat load (heat flux) was used in the model as the boundary condition at $x = L$, instead of the isolation boundary condition. As the variation of the evaporator end temperature and filling valve temperature were not linear, the conductive parasitic heat load incoming from the valve was obtained as a function of time.

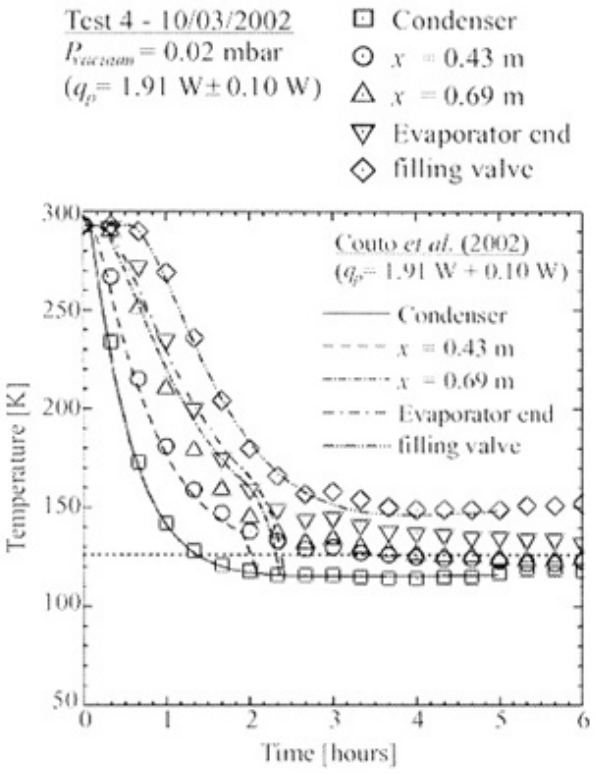

Figure 12. Transient cool-down (test IV).

The condenser temperature reached the critical temperature of the nitrogen after 1.33 h of testing, but the pressure model indicates that the vapor pressure decreased below the critical pressure only after 2 hours, when the condenser temperature was at 118 K. The theoretical model indicates that the heat pipe would prime quickly (in 25 minutes) below 118 K, but on the other hand, the experimental data indicates that there was no priming and the heat pipe was cooled only by conduction (see Fig. 13). Some possible reasons for the heat pipe startup failure are listed below:

- The vapor pressure never decreased below the critical pressure of the nitrogen due to inaccuracy of the working fluid mass weight and temperature measurement;
- The lowest temperature reached by the condenser was 116 K after 3 hours of testing. This small

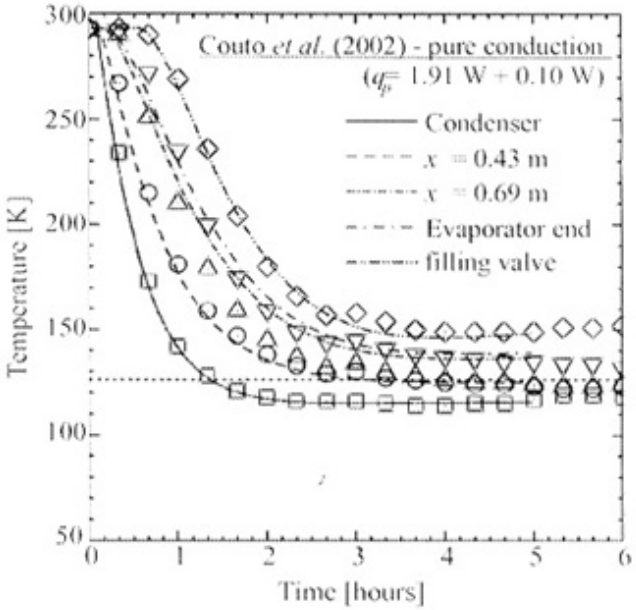

Figure 13. Pure conduction cool-down (test IV).

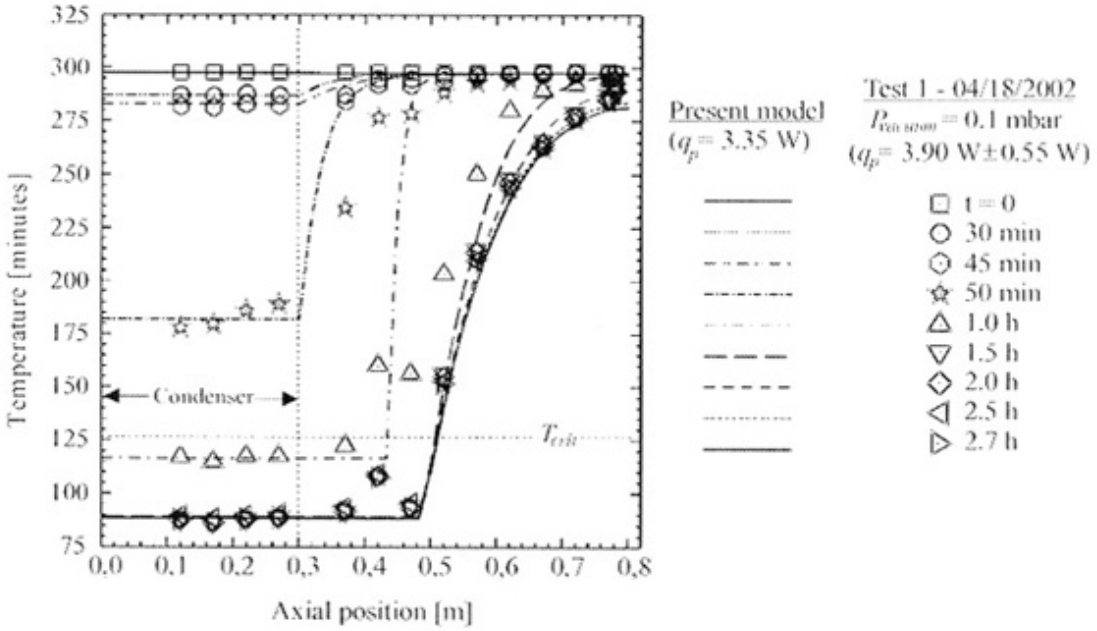

Figure 8. Temperature profiles (test I).

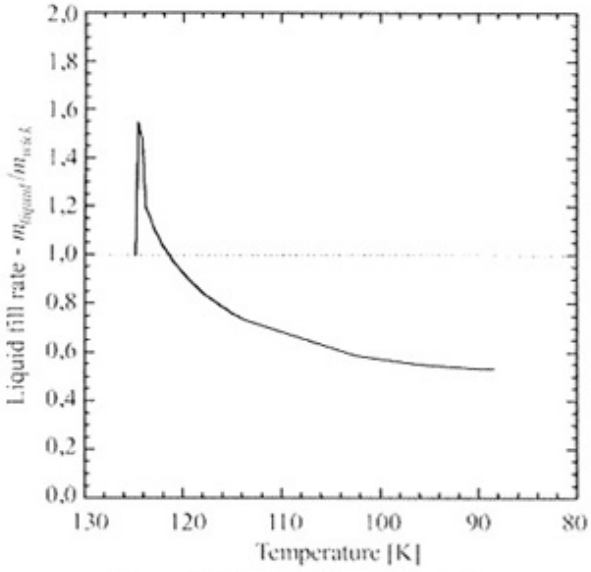

Figure 9. Liquid fill rate (test I).

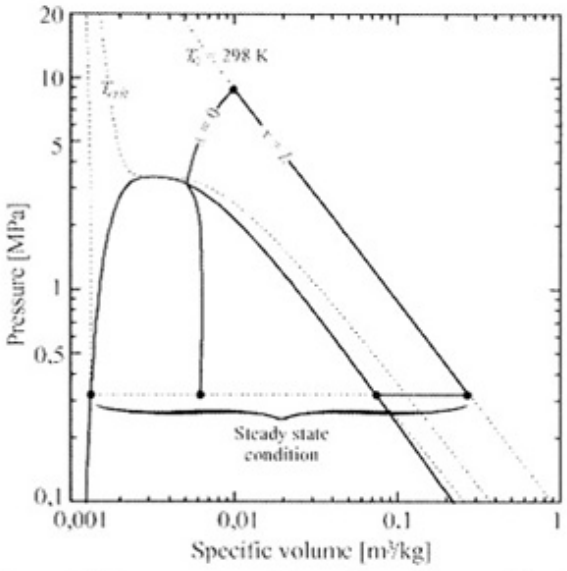

Figure 10. Pressure-specific volume diagram (test I)

load (2.46 W). Again, a non-operational steady-state condition was observed after 1 hour, but the liquid column primed 78% of the length of the heat pipe (0.62 m). Although the heat pipe was not fully primed, the improved insulation decreased the effects of the parasitic heat load, allowing the liquid column to advance inside the heat pipe. With increased insulation, the effect of the deficiency of fluid charge seems to be more evident as the heat pipe could not prime completely. The model overestimated the temperatures during transient operation, but the model was able to reproduce the steady state conditions with a good accuracy.

A third test (test III) was performed with similar conditions to those of the test II. The objective of this test was to verify the repeatability of experimental results. The vacuum chamber pressure was greater than that of the second test (10 mbar), but the experiment showed a good repeatability of results.

New tests were performed in October 3rd, 2002 (test IV). During the charging process, the heat pipe was immersed in a liquid nitrogen bath to decrease the wall temperature, because the pressure of the nitrogen gas cylinder was lower than that required for the charging process at room temperature. The heat pipe was charged with an excess of 27% of working fluid. The charged heat pipe was instrumented with 16 T-type thermocouples, and mounted at the calorimeter. The transport and evaporator sections of the heat pipe were covered with MLI, but the filling valve was not. A thermocouple was installed on the filling valve. The vacuum chamber was closed, evacuated to a pressure of 2×10^{-2} mbar, and the acquisition system was activated. Then, the calorimeter was flooded with liquid nitrogen, and no change at the vacuum chamber pressure was observed. Figure 12 shows the experimental temperature at different axial positions along the heat pipe length as a function of time obtained during this

$$q_{cond} = k_s A_s \left.\frac{\Delta T}{\Delta x}\right|_{x=0.47} = k_s A_s \frac{(T|_{x=0.52} - T|_{x=0.47})}{(0.52 - 0.47)} \quad (8)$$

With the estimations of the heat conducted from the dry region, q_{cond}, and the total heat load, Q_e, the parasitic heat load, q_p, can be obtained from Eq. (7).

It can be observed that the calorimeter was able to cool the condenser region below the nitrogen critical temperature in less than 1 hour, and after 1.5 hours the condenser achieved a steady-state average temperature of 82 K. Also, after 1.5 hours, the heat pipe achieved a non-operational steady-state condition, where only 58% of the entire length (0.47m) was primed. Two possible reasons for this non-operational condition can be listed:

- The parasitic heat loads from the environment increased the temperature gradient of the heat pipe during the startup, which was large enough to vaporize all the incoming working fluid at the liquid column leading edge in steady state conditions (x = 0.47 m). Also, liquid was vaporized along the primed length of the heat pipe due to the parasitic heat load, reducing de liquid column momentum. The combination of these two effects decreased the rewetting velocity to zero after 1.5 hours of testing;
- The fluid charge (~70% of the required fluid charge) was not sufficient to provide enough fluid for the liquid column to overcome the effects of the parasitic heat load.

In fact, the working fluid mass of a heat pipe can be written in terms of the saturated liquid and vapor densities and of the liquid and vapor volumes:

$$m_f = \rho_l V_l + \rho_v V_v = \rho_l A_l L + \rho_v A_v L \quad (9)$$

Eq. (9) provides the working fluid mass, m_f, to prime completely a heat pipe with a defined geometry (L, A_l, A_v) where the densities vary with the temperature. On the other hand, Eq. (9) can provide the maximum length L primed by a given working fluid mass as a function of the saturation temperature, which is shown in Fig. 7. The total length of the heat pipe being tested is shown in dashed line. For this calculation, the working fluid mass in the dry region and the effects of the parasitic heat load were neglected for simplification. It can be observed that a heat pipe with a deficiency of working fluid charge would never prime completely. Also, an excess of 15% in the designed working fluid mass is required for the heat pipe to prime completely below 120 K.

Figure 8 shows the axial temperature profile during the startup for different times. The model was able to predict the steady state length of the liquid column as well as the steady state axial temperature profile of the first experiment, but in general, it overestimated the transient temperatures during the startup process of the heat pipe. This is because the model considers

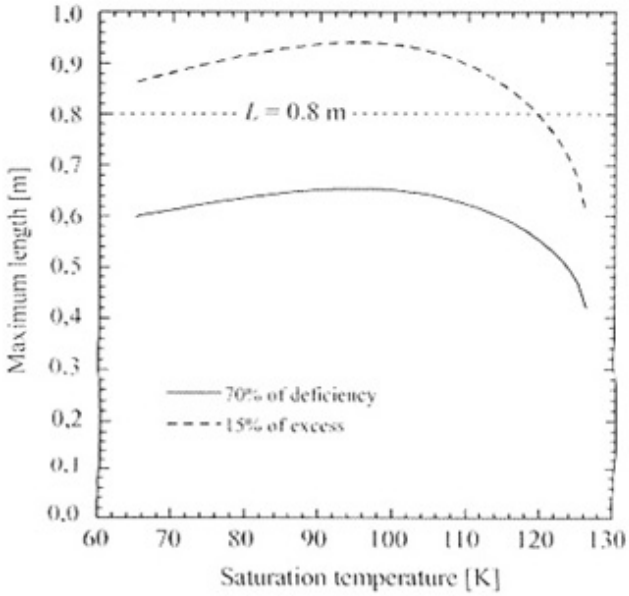

Figure 7. Maximum primed length.

that any excess of condensed liquid is accumulated in the condenser as a liquid slug (microgravity environment). In ground tests, the capillary forces cannot support a liquid slug across the vapor diameter and the excess of liquid spreads as a puddle and facilitates the priming of the heat pipe[12].

The excess working fluid during the startup is shown in Fig. 9, which presents the liquid fill rate for the test I. The liquid fill is defined as the ratio between the condensed liquid mass m_l and the mass that the wick structure can hold m_w:

$$N = \frac{m_l}{m_w} = \frac{(1-x)A_c s / v_c}{A_w s / v_l} \quad (10)$$

where x is the quality of the saturated fluid in the wetted region, A_c is the cross sectional area of the condenser (liquid + vapor), s is the position of the liquid column for a given time, A_w is the cross sectional area of the grooves, and v_c and v_l are the specific volumes of the saturated fluid in the wetted region and saturated liquid, respectively. If N = 1, the mass of liquid is enough to fill the grooves with no excess liquid. For N > 1 there is excess liquid. The theoretical pressure-specific diagram for test I, is shown in Fig. 10.

Two tests (tests II and III) followed the first one with the same fluid charge in the heat pipe. These tests were performed to evaluate vacuum leak problems at the experimental setup and thermocouple connections to the heat pipe. However, the transport and evaporator sections of the heat pipe were covered with MLI. Figure 11 shows the comparison between the experimental and the theoretical temperature profiles for different times for test II. The parasitic heat load estimated for this test was q_p = 2.95 W ± 0.49 W. For each thermocouple position, two curves were plotted: for the maximum parasitic heat load estimated (3.44 W) and for the minimum parasitic heat

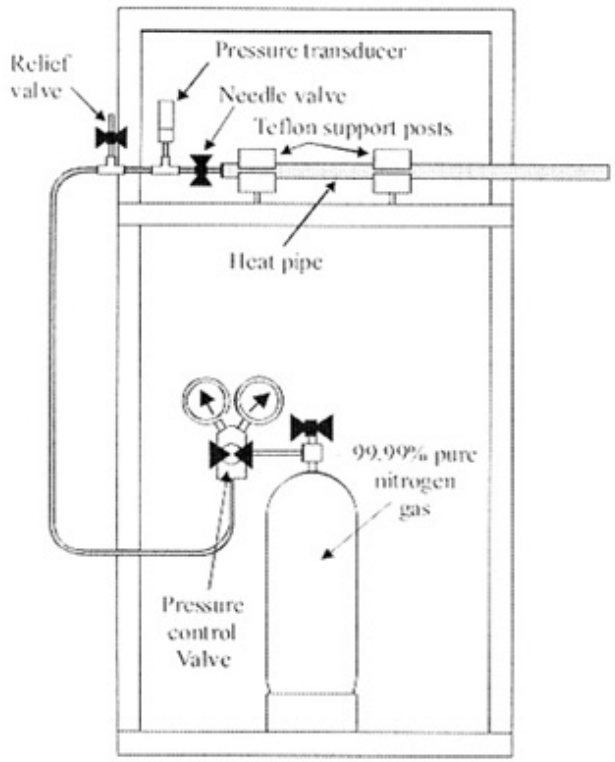

Figure 5. Charging apparatus.

nitrogen gas. The relief valve is closed and the needle valve is opened. The pressure control valve was set to a pressure higher than that required for the heat pipe charging. The pressure control valve was closed and the needle valve was closed. The relief valve was opened to vent the gas from the piping and the heat pipe is disconnected. The heat pipe was weighted again, and compared to the empty weight. The difference gives the working fluid charge. Any excess of fluid was then vented.

Heat pipe testing: The heat pipe testing consists of cooling the heat pipe condenser to a temperature below the critical temperature of the nitrogen in a vacuum environment. Initially, the heat pipe is at room temperature. The preparation for the test begins with the evacuation of the vacuum chamber using the rotary pump. When the pressure was below 2×10^{-2} mbar, the data acquisition system was activated and the calorimeter was flooded with liquid nitrogen, cooling the brass sleeve and the condenser region. The temperature of the calorimeter was constantly monitored to avoid a dry-out, which would lead to a temperature increase of the condenser. The test was finished when the largest temperature variation observed is less than 1 K/h (*i.e.*, steady-state condition).

Results and Discussion

The first test (test 1) of the nitrogen/stainless steel heat pipe constructed at the LABSOLAR/ NCTS was performed on the April 18th, 2002. After the heat pipe charging process, it was observed that there was a fluid charge deficiency of almost 30% due to leaks on the pipefittings of the charging apparatus (fixed later), added to inaccuracy of the pressure control valve.

After the heat pipe assembling in the calorimeter, the vacuum chamber was closed and evacuated to a pressure of 4×10^{-2} mbar. Leakage on the experimental apparatus prevented a lower level of vacuum. No MLI was used on the transport and evaporator section of the heat pipe. After the flooding of the calorimeter, the pressure of the vacuum chamber increased to 0.1 mbar due to differential expansion of the LN_2 feedthrough at very low temperatures.

Figure 6 shows the experimental data obtained for the test 1 of the cryogenic heat pipe. The transient temperatures during the startup for different axial positions are presented. The heat pipe achieved a non-operational steady state after 1.5 hours of testing, with the liquid column stagnating at $x = 0.47$ m.

According to the measurement uncertainty discussed before, the parasitic heat load for this experiment was estimated to be $q_p = 3.90$ W $\pm$ 0.55 W. The estimation of the parasitic heat loads was performed based on the steady state temperature measurements and based on a network thermal resistances model presented by Faghri[2]. It was considered that the primed length of the device was working as a heat pipe transporting the heat conducted from the dry region and the radiative parasitic heat load as well:

$$Q_e = q_{cond} + q_p \tag{7}$$

The total heat load, Q_e, can be estimated by using the network thermal resistance model and the temperature difference measured between the liquid column edge ($T|_{x=0.47\text{ m}}$) and the condenser section ($T|_{x=0}$). The heat conducted from the dry region, q_{cond}, was estimated based on the first two temperatures measurement in the dry region ($T|_{x=0.47\text{ m}}$ and $T|_{x=0.52\text{ m}}$):

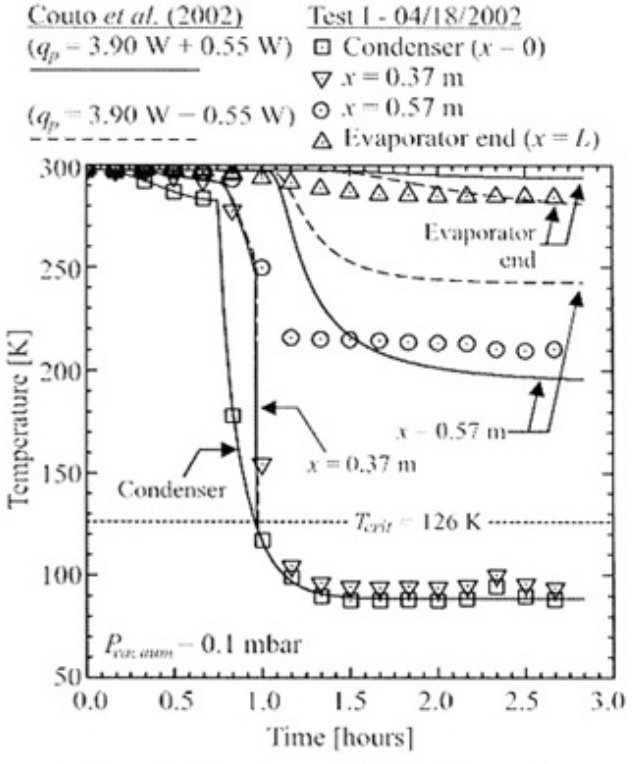

Figure 6. Transient cool-down (first test).

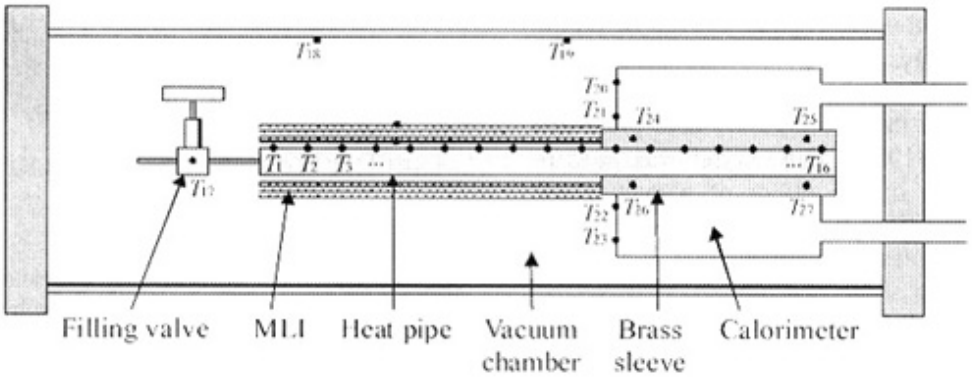

Figure 4. Thermocouple positions.

sion thermometer and saturation temperature of liquid nitrogen at atmospheric pressure (77.4 K). At the ice point temperature, the T-type thermocouples presented a random error of ±0.1 K and a systematic error of 0.2 K, while at nitrogen saturation temperature the readings were 73.8 K ± 0.3 K, showing a systematic error of –3.5 K. The variation of the systematic error and random error between 273.15 K and 77.4 K was considered linear:

$$\varepsilon_s = \left(\frac{0.2-3.5}{273.15-77.4}\right)(Y-77.4)+3.5 \qquad (1)$$

$$\varepsilon_r = \left(\frac{0.1-0.3}{273.15-77.4}\right)(Y-77.4)+0.3 \qquad (2)$$

where Y is the measured temperature recorded by the data acquisition system. The corrected value of the measured temperature is given by:

$$T = Y + \varepsilon_s \pm \varepsilon_r \qquad (3)$$

where ε_s and ε_r are the systematic and random errors.

The measurement of temperature at cryogenic levels is very difficult to be performed. At such low level of temperature, the heat conduction by the thermocouple wires can affect the measured data. The data acquisition system is at room temperature, and to avoid the heat conduction from the data acquisition system, the thermocouple wires are thermally grounded at the calorimeter. The heat conduction through the grounded thermocouple wires can be calculated by:

$$Q_{fio} = n\frac{\pi d_w^2 \Delta T}{4L}\left(k_{Cu} + k_{Co}\right) \qquad (4)$$

where n is the number of thermocouples, d_w is the wire diameter, ΔT is the difference between the local heat pipe temperature and the calorimeter temperature, L is the wire length and k_{Cu} and k_{Co} are the conductivity of the copper and the constantan wires. For a temperature difference of 23 K between the calorimeter and the heat pipe, the heat transferred through the thermocouple wires is 1×10^{-3} W, while at 100 K the heat transport capacity of the heat pipe is 2 W. Therefore, the heat lost by conduction through the thermocouple wires is less than 0.05% of the heat pipe transport capacity, thus being negligible.

Experimental Procedure:

Before being tested, the heat pipes is cleaned, assembled and charged. End-caps were machined and welded to the heat pipe container. The inner surface of the end-caps have a hemispherical shape to avoid sharp corners, which are sensitive to cracking due to the high internal pressure of the heat pipe at room temperature. A filling tube (1/8" ∅ external diameter, 50 mm long) was also machined.

Heat pipe cleaning: The heat pipe container, metal screen, end-caps and filling tube were cleaned in an ultrasonic cleaning equipment using trichloroethane for degreasing and solid particle removal. After cleaning, a passivation process was performed. This process consists in immersing the parts in a solution of 60% nitric acid and deionized water for 2 hours. After the passivation, the parts were wrapped in plastic to prevent contamination prior to assembly.

Heat pipe assembling: A metal screen wick mesh 160 was wrapped inside the heat pipe container in order to obtain a wick structure with 8 layers. The material of the metal screen is AISI 316 stainless steel. The end-caps and filling tube were welded to the container by a TIG process. The heat pipe was filled with argon gas to prevent oxidation during the welding process. After welding, the heat pipe was cleaned again as described before. A Swagelok® valve was connected to the filling tube to seal the heat pipe after charging.

Heat pipe charging: The heat pipe was charged with 99.99% pure nitrogen. The process was performed at room temperature, where Fig. 5 shows a schematic for the charging process. The heat pipe was connected to an Edwards® RV8 rotary vacuum pump for evacuation to a pressure of 2×10^{-3} mbar. The valve was closed and the pump was disconnected. The heat pipe was weighted empty, prior to the charging process. After weighting, the heat pipe was connected to a high-pressure cylinder containing pure nitrogen gas, a pressure control valve, a pressure transducer (Edwards® APG-M) and a pressure relief valve. With the needle valve closed, the relief valve and the pressure control valve are opened to flood the piping with

As the temperature of the condenser continues to decrease (line 5a – 5b – 5c), more liquid is condensed where the liquid eventually advances towards the evaporator. The process continues until the heat pipe is completely primed and the thermodynamic state at the wick structure and vapor region is given by points 6a and 6b, respectively.

The startup model presented by Couto *et al.*[4] compared favorably with the microgravity data presented by Brennan *et al*[12] (1993). This model was used to perform an analysis of the effect of parasitic heat loads on the supercritical startup. From the results it was found that an excessive parasitic heat load could cause a partial startup of the heat pipe.

For additional validation of the proposed startup process and of the theoretical model, ground tests of a nitrogen/stainless steel cryogenic heat pipe were performed. Although the model did not consider the effects of the gravitational field, the comparison provides a good insight to the supercritical startup of cryogenic heat pipes.

Experimental Analysis

The experimental analysis was performed at the NCTS facilities, at the Federal University of Santa Catarina, Brazil. The experiment consists of testing a nitrogen/stainless steel cryogenic heat pipe in a vacuum chamber using a calorimeter filled with liquid nitrogen to cool the condenser region. The experimental setup allows horizontal and tilted tests of heat pipes under a high vacuum environment ($P_{abs} < 1 \times 10^{-2}$ mbar).

Experimental Facility:

The experimental setup used for the tests of the stainless steel/nitrogen cryogenic heat pipe consists of a horizontal vacuum chamber (1200 mm long, ∅200 mm ID) and a calorimeter (2.2 liters) through which flows liquid nitrogen. Figure 3 shows the vacuum chamber schematic. To accommodate different heat pipe geometries, the calorimeter has an internal cavity with a diameter larger than the external diameter of the heat pipes. A brass sleeve fills the gap between the calorimeter and the heat pipe, to provide a prescribed temperature boundary condition at the condenser region. Latter, a new calorimeter (2.4 liters) was developed to allow direct contact between the liquid nitrogen and the heat pipe condenser section, providing more cooling capacity to the experimental setup.

The vacuum chamber was connected to an Edwards® RV8 rotary vacuum pump. The pressure in the vacuum chamber was monitored using an active pressure gauge Edwards® APG-M connected to an Edwards® AGD display. At one side of the vacuum chamber, there is a feedthrough for 36 T-type thermocouples and two pairs of electrical connections. At the other side of the vacuum chamber, there is a pair of feedthroughs where the liquid nitrogen (LN2) flows to the calorimeters. Two brass sleeves surround the condenser region of the heat pipe, to fit inside the calorimeter.

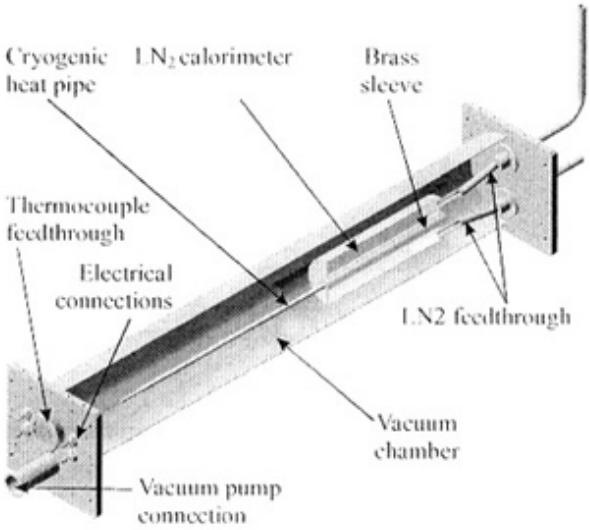

Figure 3. Vacuum chamber schematic.

Heat Pipe Design Summary and Instrumentation:

The nitrogen/stainless steel cryogenic heat pipe (CryoNHP) design, and summarized at Table 1. The condenser region of the heat pipe was placed in the calorimeter, while the remaining length was covered with a multi-layer insulation (MLI) composed of 10 layers to avoid radiative parasitic heat loads. A Hewlett-Packard® 34970A Data Acquisition Unit was used to monitor the temperature of 16 Omega® T-type AWG40 thermocouples that were installed at the external wall of the heat pipe (see Figure 4). Also, the temperature of the following items was monitored for future parameter estimation:

- Filling valve of the heat pipe;
- Vacuum chamber inner wall;
- Outer and inner layer of the heat pipe's MLI;
- Brass sleeves;
- Calorimeter.

Table 1. CryoNHP design summary (Couto[14]).

Tube material:	AISI 304 Stainless Steel
Tube dimensions:	
Outer diameter	19.05 mm (3/4")
Wall thickness	1.3 mm
Lengths:	
Evaporator	0.30 m
Condenser	0.30 m
Transport section	0.20 m
Nitrogen charge:	31.1 g
Maximum heat transport capacity:	2.2 W.m (at 82 K)
Wick structure:	Metal screen
Mesh	160
Number of layers	8
Thickness	1.676 mm

Uncertainty Analysis:

The thermocouples were calibrated at two reference temperatures: ice point temperature at atmospheric pressure (273.15 K ≡ 0°C) using an Hg preci-

load. This parasitic heat load is provided by the radiation heat transfer between the heat pipe and the spacecraft structure or heat loads from the space environment. According to Couto *et al.*[4], depending on the initial condition of the heat pipe, the working fluid at the condenser region may achieve a subcooled condition first than a saturated condition. The current investigation consider two cases for the initial condition: the initial specific volume of the heat pipe (void volume of the heat pipe/working fluid mass) is much larger than the critical specific volume of the working fluid ($v_{HP} >> v_{crit}$), or the specific volume is less or near the critical specific volume ($v_{HP} < v_{crit}$ or $v_{HP} \sim v_{crit}$).

Case 1 - $v_{HP} >> v_{crit}$: The first case can be understood by observing the pressure-specific volume diagram shown in Figure 1. At the beginning of the process the heat pipe is considered to be isothermal at T_0, where the initial condition of the heat pipe is represented by point 1 in the supercritical region. As the start-up proceeds, a horizontal line represents the thermodynamic state of the heat pipe, where the pressure is assumed essentially uniform in the heat pipe at any point in time. This line lowers as the internal pressure decreases. In Fig. 1, point 2a represents the specific volume at the condenser end, and point 2b represents the specific volume at the evaporator end. It is important to observe, at the thermodynamic state 2, that the vapor pressure is lower than the critical pressure, but the temperature of the condenser remains above the critical temperature. As the temperature of the condenser continues to decrease, the condenser will enter the superheated region when the temperature of the condenser decreases below the critical temperature, or $T_c < T_{crit}$. The condensation process will start when the temperature of the condenser equals the saturation temperature (point 3b) at the vapor pressure at that point in time [$T_c = T_{sat}(P_v) \equiv P_v = P_{sat}(T_c)$]. At this moment, liquid condenses at the wick structure (point 3a), and saturated vapor fills the vapor space at the condenser region (point 3b). The remaining length of the heat pipe remains dry in a superheated condition (line 3b – 3c). As the temperature of the condenser continues to decrease (line 4a – 4b – 4c), more liquid condenses on the wick structure, which eventually advances towards the evaporator via the wick structure. The process continues until the heat pipe is completely primed, and the thermodynamic state at the wick structure and vapor space is given by points 5a and 5b, respectively.

Case 2 - $v_{HP} < v_{crit}$ or $v_{HP} \sim v_{crit}$: The second case can be figure out by observing the pressure-specific volume diagram shown in Fig. 2. In this case, as the startup progresses, the condenser will reach the critical temperature before the vapor pressure decreases below the critical pressure, at point 2a. At this point, the vapor inside the condenser region changes from supercritical fluid to subcooled liquid because its temperature is below the critical temperature, but the vapor pressure is still greater than the critical pressure ($T_c < T_{crit}$ and $P_v > P_{crit}$). The subcooled liquid fills the wick structure and the vapor space in the condenser region forming a liquid slug. As the temperature of the condenser decreases, the subcooled liquid slug extends into the transport section until the vapor pressure equals the critical pressure at point 3c. At this point, the leading edge of the subcooled slug will be at a critical condition once the local temperature and vapor pressure are equal to the critical temperature and pressure ($T|_{x=s-Lc} = T_{crit}$ and $P_v = P_{crit}$). From this point on, the length of the subcooled liquid slug decreases until the condenser temperature reaches the saturation pressure at that point in time [$T_c = T_{sat}(P_v)$] at point 4a. At this point, the condenser region is filled with saturated working fluid: saturated liquid at the wick structure (point 4a) and saturated vapor at the vapor space (point 4b). The remaining length of the heat pipe remains dry, in a superheated condition.

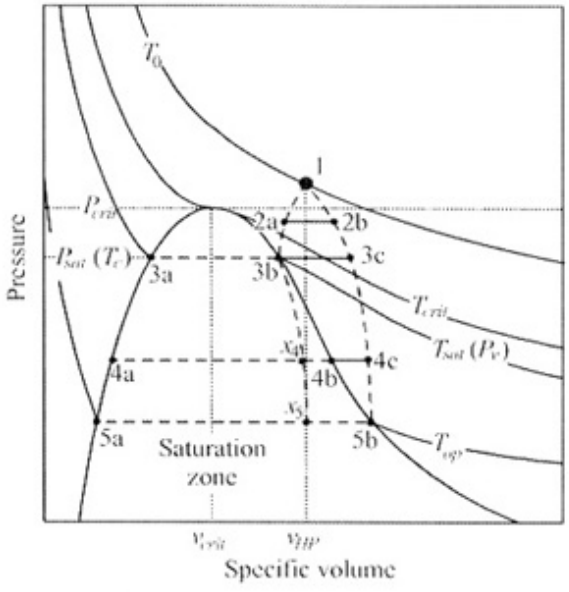

Figure 1. Pressure-specific volume diagram for $v_{HP} >> v_{crit}$.

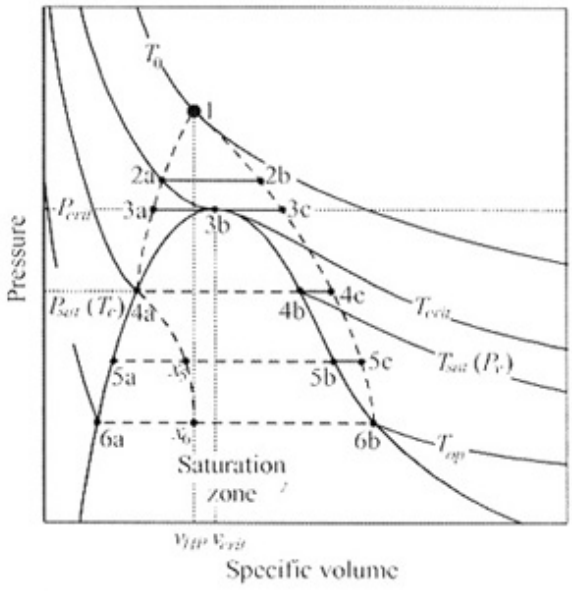

Figure 2. Pressure-specific volume diagram for $v_{HP} < v_{crit}$.

for the ground test of cryogenic heat pipes. A nitrogen/stainless steel cryogenic heat pipe (CryoNHP) was designed and the results of the ground tests are presented. The technology of cryogenic heat pipes is under investigation at NCTS[9] in order to develop a passive cryogenic thermal control device for the payload of the Brazilian satellites. This project is funded by the Brazilian Space Agency (AEB) and Brazilian Council for Research and Development (CNPq) in the frame of the University Program for Space Development (UNIESPAÇO)[10].

Literature Review

Unlike low and medium temperature heat pipes, a cryogenic heat pipe typically starts from a supercritical state. The entire heat pipe must be cooled below the saturation temperature of the working fluid for nominal operation. Previously, Colwell[11], Brennan *et al.*[12], Rosenfeld *et al.*[13], Yan and Ochterbeck[3] and Couto[14] have discussed the start-up process of cryogenic heat pipes.

Colwell[11] (1977) presented a numerical analysis of the transient behavior of a nitrogen/stainless steel cryogenic heat pipe with circumferential screen wick structure and composite central slab. The three-dimensional model assumed constant properties, but did not account for the fluid dynamics of the working fluid. Although provisions for simulating a supercritical start-up were included, the author only presented results for the start-up of the heat pipe with an initial temperature already below the working fluid critical temperature.

A microgravity experiment for two different aluminum/oxygen axially grooved heat pipes was conducted by Brennan *et al.*[12] (1993). The experiment was flown aboard the STS-53 space shuttle mission in December 1992. Reliable start-ups in flight of the two heat pipes were performed, but the start-up process in microgravity was slower than that obtained in ground tests. This is because in a microgravity environment the condensation of the working fluid develops a liquid slug in the condenser region. In ground tests the excess liquid forms a puddle along the wick structure due to the effects of the gravitational forces.

Rosenfeld *et al.*[13] (1995) presented a study of the supercritical start-up of a titanium/nitrogen heat pipe. The test was performed during mission STS-62 (March, 1994). This heat pipe achieved a non-operational steady state thermal condition during microgravity tests. Only 30 % of the heat pipe length cooled below the nitrogen critical point, but the vapor pressure was still above the critical pressure. However, Rosenfeld *et al.*[13] observed that in ground tests, the titanium/nitrogen heat pipe underwent start-up successfully. The authors concluded that, with the addition of parasitic heat loads, the thermal conduction of the titanium/nitrogen heat pipe was insufficient to allow for the internal pressure to decrease below the critical pressure of nitrogen when in microgravity. The successful start-up during ground tests was due to enhanced thermal transport of the gravity-assisted priming effects. These tests highlighted the significance of the parasitic heat loads, as the heat pipe start-up failure probably would not occur in microgravity if the heat leaks had been significantly reduced.

Yan and Ochterbeck[3] (1999) presented a one-dimensional transient model for the supercritical start-up of cryogenic heat pipes. The start-up process was divided into two stages. In the first stage, the heat pipe is cooled by pure heat conduction, and the vapor temperature at the condenser is greater than the critical temperature ($T_c > T_{crit}$). The cooling effect resulting from the condenser heat rejection is not immediately propagated through the heat pipe, but it is confined to a region extending from the condenser to some penetration depth δ. Beyond δ, the temperature gradient is zero. When the penetration depth equals the heat pipe length, the cooling effect of the condenser has propagated over the entire heat pipe.

In the second stage, the vapor temperature is lower than the critical temperature ($T_c < T_{crit}$). When the condenser temperature is lower than the critical temperature and the internal pressure is lower than the critical point, the vapor begins to condense in the condenser section. The advancing liquid layer is subjected to a capillary driving force that is induced by surface tension and opposed by the wall shear stress, as it advances with an average velocity that will vary with respect to the length of the liquid layer. With increasing time, the liquid average velocity in the condenser increases. The liquid front will advance, until the heat pipe achieves its operational steady state, assuming sufficiently low heat leaks. This model compared favorably with the microgravity experimental data presented by Brennan *et al.*[12], but it did not include effects of the parasitic heat load over the heat pipe working fluid. Also, this model did not account for the working fluid mass distribution and, therefore, it was not possible to estimate the liquid slug length observed by Brennan *et al.* (1993).

Couto *et al.*[4,14] presented a one-dimensional model, which included the effects of the parasitic heat load over the cryogenic heat pipe supercritical startup. Also the vapor pressure and density gradient of the working fluid were determined based on the temperature gradient and the total working fluid mass. The supercritical startup process described by Couto *et al.*[4] is very similar to that described by Yan and Ochterbeck[3], but it was shown that a subcooled condition can exist in the condenser prior to the condensation process start, depending on the vapor pressure. The initial temperature of the heat pipe considered is above the critical temperature, and the boundary condition at the condenser region is a specified time-variable temperature. This condition is consistent with most experiments in the literature, which use cryocoolers to provide the required heat rejection at the condenser region. The remaining length of the heat pipe (adiabatic and evaporator regions) is considered to be under the influence of a radiative parasitic heat